Journal of Materials Chemistry A

Accepted Manuscript

ROYAL SOCIETY OF CHEMISTRY

www.rsc.org/materialsA

Journal Name

ARTICLE

Flexible Graphene/Silicon Heterojunction Solar Cells

Kaiqun Ruan, Ke Ding, Yuming Wang, Senlin Diao, Zhibin Shao, Xiujuan Zhang* and Jiansheng Jie*

Received 00th January 20xx,
Accepted 00th January 20xx

DOI: 10.1039/x0xx00000x

www.rsc.org/

Graphene/silicon heterojunction solar cells have attracted intensive research interests owing to the simple device structure as well as the low-cost process capability at room temperature. However, the use of thick silicon substrates hampers their application in flexible solar cells, despite the high flexibility of graphene. Here, we report the construction of flexible graphene/silicon solar cells by taking advantage of the high flexibility of ultrathin Si substrates. Through systemically optimizing the device structures, including performing surface passivation on Si, inserting a layer of poly(3-hexylthiophene) (P3HT) as an electron blocking layer, and controlling the layer number and doping of graphene, a power conversion efficiency of 8.42% was successfully achieved. The photovoltaic characteristics of the graphene/ultrathin silicon heterojunctions were further evaluated under bend conditions, revealing their excellent flexibility and durability. Our work paves the way toward low-cost, high-performance, flexible graphene/silicon heterojunction solar cells.

Introduction

Currently, crystalline silicon (c-Si) based solar cells have dominated large portions of the commercial solar cell market on account of material abundance, non-toxicity, superior reliability and mature technology. However, the high cost of c-Si solar cells, mainly originating from raw material consumption and complicated fabrication processes, still hinders their ubiquitous applications. In addition, conventional c-Si based solar cells are heavy and fragile due to the large thickness (~150 μm), which are not suitable for integrating with infrastructures of various shapes and sizes where lightweight and flexibility are important.[1] Therefore, the new conceptual solar cells based on flexible thin c-Si substrates are rising and appealing, which draw considerable attention in recent years.[2-4] On the other hand, the use of thin Si substrates can be an advantage for the minority carriers that have a short diffusion length, which can contribute to the reduction of electron-hole recombination.[5] Nevertheless, large-scale fabrication of thin c-Si substrates is precondition for assembling photovoltaic devices and remains a challenge. So far, there have been three main methods to fabricate thin c-Si solar cells, including epitaxial growth and layer transfer,[6, 7] etch-release method,[8, 9] and exfoliating from bulk silicon wafer, [10, 11] but their process sequences are complicated and the sizes of thin c-Si substrates are also restricted. Recent advances demonstrated the fabrication of large-area ultrathin c-Si (thickness <10 μm) at wafer scale with good processability *via* alkaline etching approach, which makes a further step toward thin c-Si based solar cells.[12] However, it is worth noting that most of the flexible thin c-Si based solar cells were fabricated by making conventional p-n junctions which are realized through a number of steps, such as high temperature

Institute of Functional Nano & Soft Materials (FUNSOM), Collaborative Innovation Center of Suzhou Nano Science and Technology, Jiangsu Key Laboratory for Carbon-Based Functional Materials & Devices, Soochow University, Suzhou, Jiangsu 215123, P. R. China.

† Electronic Supplementary Information (ESI) available: Cross-sectional view SEM images of ultrathin Si substrates with different thickness and their corresponding photographs under bending; *J-V* curves of a typical device w/o P3HT layer; See DOI: 10.1039/x0xx00000x

diffusion and annealing. The complicated processes will inevitably increase the energy consumption, the cost of the devices, as well as the probable damage to thin c-Si substrates. In order to simplify the fabrication procedures and reduce the cost of thin c-Si solar cells, heterojunctions that combine abundant photovoltaic materials with thin c-Si substrates at room temperature have been developed,[13-15] but a favorable efficiency has not been achieved yet.

Graphene transparent electrodes have attracted a great deal of research interests, because of the extraordinary properties, including superior electrical conductivity, outstanding mechanical flexibility, high transparency and good chemical stability.[16-21] The chemical vapour deposition (CVD) method can achieve large-area growth of high-quality graphene,[22] greatly facilitating its applications in various areas such as light-emitting diodes (LEDs), touch screens, and solar cells.[23-28] Recently, the graphene/c-Si hetreojunction solar cells have simulated many research activities because of its easy fabrication, low-cost, and remarkable photovoltaic performance.[29] The graphene/c-Si solar cells showed a low power conversion efficiency (PCE) of 1.5% at early stage,[30] and many progresses have been achieved to make the efficiency more promising.[31-37] For instance, Miao et al. improved the efficiency significantly from 1.9% to 8.6% by appropriate chemical doping.[32] Through surface passivation and band engineering, we demonstrated a PCE of 10.56%.[34] Shi et al. adopted a layer of TiO_2 as an antireflection coating to enhance the efficiency to 14.5%.[36] However, the above researches were made on the basis of thick c-Si wafer, flexible graphene/c-Si solar cells are yet to be demonstrated.

Herein, we reported the construction of flexible graphene/silicon heterojunction solar cells by combining graphene with flexible ultrathin c-Si that was fabricated by etching method in concentrated alkaline solution. A thin layer of poly(3-hexylthiophene) (P3HT) was inserted between graphene and ultrathin c-Si as an electron blocking layer to suppress the interface carrier recombination. The c-Si thickness and graphene layer number dependent device performance were further investigated. With optimum graphene layer number as well as effective surface passivation on ultrathin c-Si surface, a PCE of 8.42% has been achieved under a c-Si thickness of 40 μm. The devices also exhibited excellent stability under bending conditions. Given the low-cost solution processed capability, our results open up a new possibility for c-Si based flexible solar cells.

Experimental details

Fabrication of ultrathin c-Si

N-type double-side polished single-crystalline Si wafers (Orientation (100), resistivity 1-3 Ωcm, thickness 390 μm) were used in our experiments. First, the wafers were cut into several pieces and then cleaned with deionized (DI) water, acetone, and ethanol each for 10 min by ultrasonic. After cleaning, the c-Si substrates were etched by concentrated potassium hydroxide (KOH) solutions (50 wt %) at 90 ^oC. By tuning the etching time from 100 min to 90 min, the thin c-Si substrates with thicknesses varying from 4 μm to 40 μm could be obtained. Finally, the as-fabricated ultrathin c-Si substrates were further cleaned with diluted hydrochloric acid (HCl) solution and DI water to remove any etchant residues.

Synthesis and transfer of graphene

Graphene was synthesized using Cu foil as catalytic substrate by CVD method. After annealing the Cu foil in tube furnace at 1040 ^oC for 60 min, a reaction gas mixed with CH_4 (10 SCCM) and H_2 (100 SCCM) was introduced into the furnace for 30 min. Then the growth of graphene was carried out. After that, the furnace was cooled down quickly. The as-prepared monolayer graphene film on Cu foil was transferred onto the ultrathin Si substrates by a poly(methyl methacrylate) (PMMA)-supported etching method, in which 8% PMMA solution was first spin-coated onto the graphene film and then the underlying Cu substrate was etched off by concentrated $FeCl_3$ solution. Multi-layer graphene films were prepared by using a layer-by-layer transfer method (LBL).[38] Eventually, the graphene films were rinsed with DI water for several times to eliminate surface contaminants.

Fabrication of photovoltaic devices

The obtained n-type flexible ultrathin c-Si substrates were firstly washed by using acetone, ethanol, DI water each for 15 min, followed by bathing with a heated piranha solution (H_2SO_4 : H_2O_2 = 3 : 1, V/V) to further remove residuals. Then, CH_3-terminated surface modification was performed to saturate dangling bonds of the ultrathin c-Si by a two-step chlorination/alkylation method in a glove box.[39, 40] It was demonstrated that surface CH_3 modification can offer excellent surface passivation on Si.[33, 41] After that, 10 nm P3HT that used as electron blocking layer was spin-coated on the ultrathin c-Si substrate. In order to define functional area accurately as well as avoid the short circuit of the device, a polydimethylsiloxane (PDMS) layer (10 μm thick) with a 4 mm hole in the center was attached onto the ultrathin c-Si substrate. The PDMS layer could sever as an insulator layer between substrate and top electrode. Afterwards, the graphene film was transferred onto the ultrathin c-Si substrate; the contact of graphene with ultrathin c-Si within the hole region of PDMS layer forms the graphene/silicon heterojunction. Finally, mm-thick Ag paste was adhered on the top surface of graphene around the centre hole on PDMS layer, working as a front contact electrode for the following photovoltaic measurements, and an indium-gallium (In-Ga) eutectic alloy was pasted on back side of the device as rear electrode to n-type Si substrate due to its low work function.

Characterizations and measurements

Thickness of the as-fabricated ultrathin c-Si substrates was checked by scanning electron microscope (SEM, FEI Quanta 200FEG). The absorption spectra of the ultrathin c-Si with different thicknesses were detected by UV-Vis spectrometer (Perkin-Elmer Lambda 750), by which the optical transmittance of graphene films was also measured. The graphene quality was confirmed by Raman spectroscope (Horbia Jobin-Yvon Labram HR800). The photovoltaic characteristics of the flexible graphene/c-Si heterojunction solar cells were tested by a Keithley 2612 source meter and a solar Newport 91160 simulator under AM 1.5G at an irradiation intensity of 100 mW/cm^2, calibrated by a Newport standard Si solar cell (91150). Newport monochromator 74125 and power meter 1918 with Si detector 918D were used to measure the external quantum efficiency (EQE).

Results and discussion

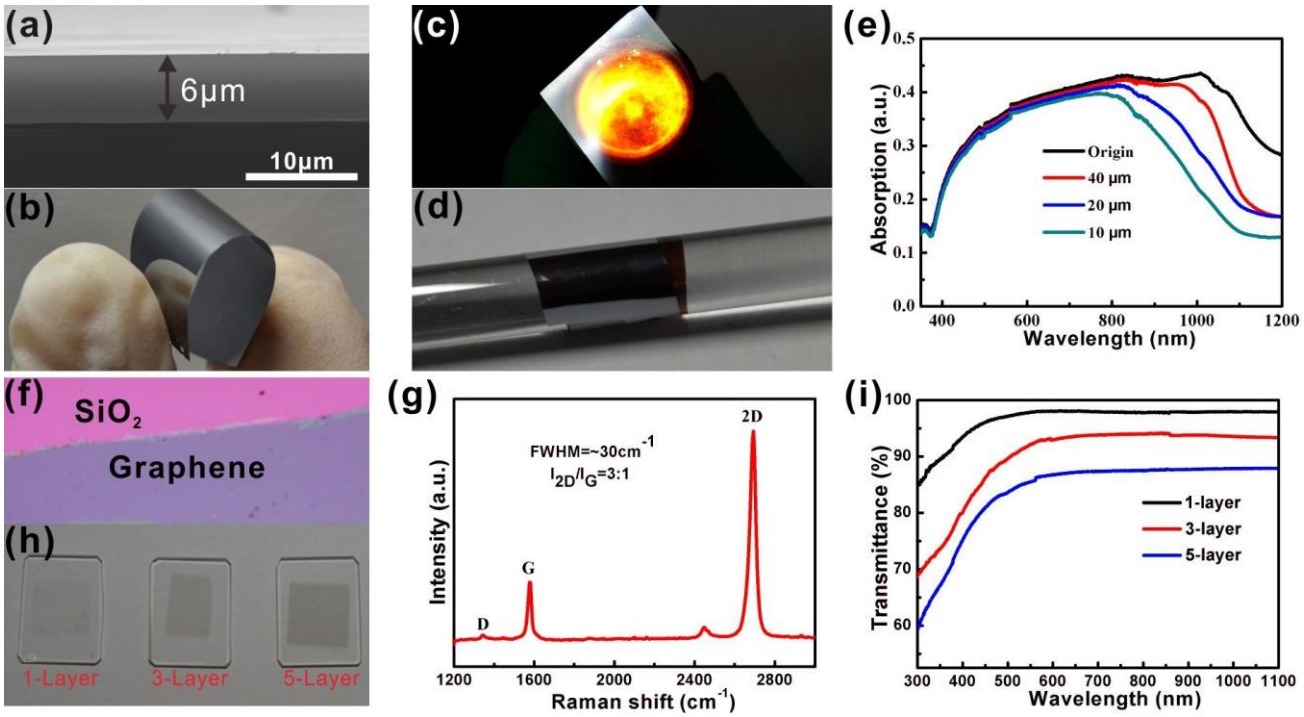

Figure 1. (a) Cross-sectional view SEM image of a 6 μm-thick Si substrate. (b) Photography of the 6 μm-thick Si under bending condition. (c) Photography of a 4 μm-thick Si illuminated by a white light source from the backside. (d) Photography of the 4 μm-thick Si that was wrapped around a glass rod with a diameter of 6 mm. (e) Light absorption spectra of ultrathin Si substrates with varied thickness of 10, 20, and 40 μm, compared with that of the original bulk Si wafer (390 μm). (f) Optical microscope image of monolayer graphene on SiO_2 (300 nm)/Si substrate. (g) Photography of 1, 3, and 5 layers graphene films on quartz substrates. (h) Raman spectrum of the as-transferred monolayer graphene. (i) Transmittance spectra of the graphene films with varied layer numbers of 1, 3, and 5.

The as-cut original silicon substrate was immersed into heating 50 wt% KOH solutions at 90 °C. The etching of KOH on Si led to the release of a large amount of gas *via* the reaction : $Si+2KOH+H_2O=K_2SiO_3+2H_2\uparrow$. By controlling the etching duration time, ultrathin Si substrates with different thicknesses were obtained. Figure 1a presents the cross-sectional SEM image of a 6 μm-thick ultrathin Si substrate, which can be bent to almost 180 °(Figure 1b), demonstrating the good flexural flexibility. The bending capacities of ultrathin c-Si substrates with various thicknesses are shown in Figure S1 in Supporting Information, verifying that the mechanical flexibilities of the ultrathin c-Si substrates depend on their thickness with thinner Si substrate showing better flexibility. As we known, light absorption of c-Si substrate is insufficient when its thickness is below 180 μm. In particular, when the thickness is decreased below 10 μm, the ultrathin c-Si substrate becomes optically transparent in long wavelength range, as revealed in Figure 1c, showing a 4 μm-thick ultrathin c-Si substrate with underneath white light illumination.

Moreover, the 4 μm-thick ultrathin c-Si substrate also exhibits excellent robustness against bending so that it can be warpped around a glass rod with a diameter of 6 mm (Figure 1d), further demonstrating the remarkable flexibility of ultrathin c-Si substrates. In addition, in order to gain insight into the light absorption of the as-fabricated ultrathin c-Si substrates, light absorption of ultrathin c-Si substrates with different thicknesses was investigated (Figure 1e). Compared with the original bulk c-Si, the absorption of ultrathin c-Si substrates is almost same at short wavelength region, but with the decrease of thickness, the thinner c-Si shows lower light absorption at visible and infrared regions.

Figure1f displays the optical microscope image of monolayer graphene transferred onto a SiO_2 (300 nm)/Si substrate. The colour contrast between the graphene film and the substrate indicates that the monolayer graphene is intact and uniform. Furthermore, Raman spectrum was utilized to evaluate the quality of the graphene film, as shown in Figure 1g. One can note that there are two characteristic bands: G band centered at 1580 cm^{-1}, associated with the crystallinity of graphene, and 2D band centered at 2700 cm^{-1}, originated from photon resonance. In contrast to the obvious G band and 2D band, the intensity of D band at 1350 cm^{-1} is extremely low, indicating that there are scarcely any disorders and defects.

Journal Name

ARTICLE

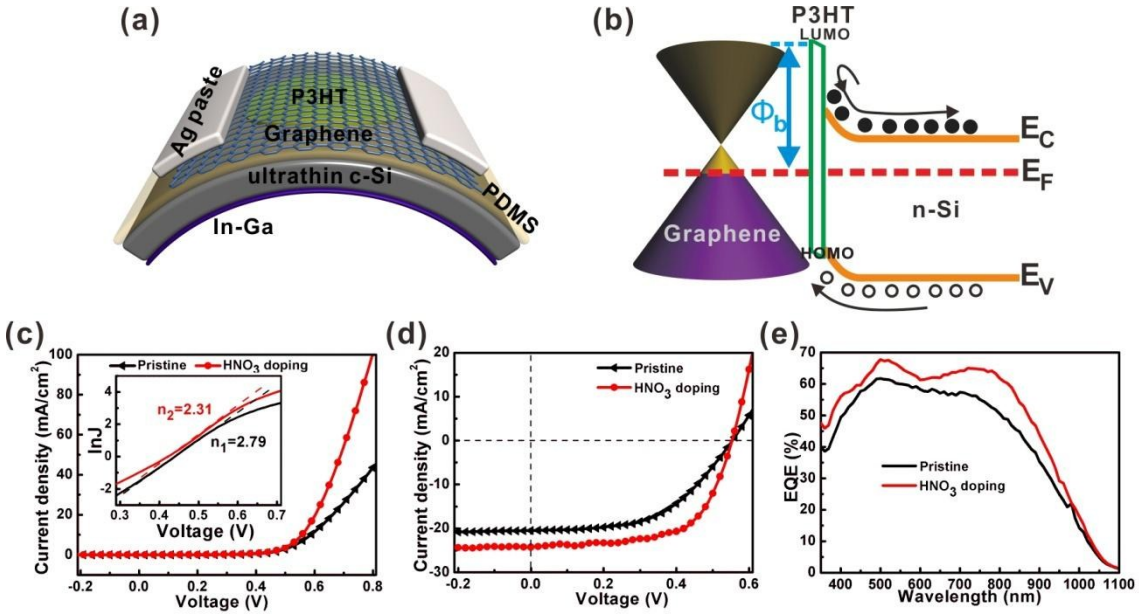

Figure 2. (a) Schematic illustration of the flexible garphene/ultrathin c-Si heterojunction solar cell. A thin layer of P3HT was inserting between graphene and c-Si as electron blocking layer. (b) Energy band diagram of the graphene/ultrathin c-Si heterojunction solar cell. (c) Dark *J-V* curves of a typical device with and without HNO_3 doping. Inset shows the corresponding dark ln*J-V* curves. (d) *J-V* curves of the device with and without HNO_3 doping under AM 1.5G illumination. The thickness of the ultrathin silicon substrate is 40 μm. (e) EQE spectra of the device with and without HNO_3 doping.

The intensity ratio of I_{2D}/I_G is equal to 3 with full width at half maximum (FHWM) being about 30 cm^{-1}, which suggests that the CVD grown graphene on copper foil is monolayer. The optical characteristic was also investigated by transferring graphene onto quartz substrates (Figure 1h), revealing that the transmittance decreases with increasing layer number of graphene film. This trend is confirmed by the optical transmittance measurements, as shown in Figure 1i. However, the conductivity of graphene film is improved remarkably with layer number from 648 Ω/□ for 1-layer graphene to 180 Ω/□ for 5-layer graphene.[34] Evidently, the opposite trend indicates that there must be a trade-off between the transparency and conductivity of graphene film for transparent electrode applications.

Schematic illustration in Figure 2a shows the device structure of flexible graphene/c-Si heterojunction solar cell. The detailed fabrication process is described in experimental section. In order to define functional area of the device and avoid the short circuit as well, a PDMS membrane with 4 mm diameter hole at centre was adhered onto the ultrathin c-Si substrate as an insulator layer. Moreover, a thin layer of P3HT was inserted between graphene and c-Si by spin-coating as an electron blocking layer, as investigated in our previous studies.[33] The underlying physical mechanism of the graphene/P3HT/c-Si sandwich structured heterojunction can be understood from the energy band diagram, as depicted in Figure 2b. It is known that the conduction band (E_C) and valence band (E_V) of c-Si are 4.05 eV and 5.17 eV, respectively, while the lowest unoccupied molecular orbital (LUMO) and the highest occupied molecular orbital (HOMO) of P3HT are 3.2 eV and 5.1 eV, respectively. Therefore the offset of E_C-LUMO (~0.8 eV) exhibits a large potential barrier for electrons transportation from c-Si to graphene, which facilitates the separation of photo-generated electron-hole pairs and thus minimizes the surface carrier recombination at graphene and Si interface. In addition, junction barrier height (Φ_b) between graphene and n-Si will be increased upon the use of P3HT layer, contributing to the enhanced device performance, as discussed later. On the other hand, p-type doping on graphene is accomplished by using concentrated nitric acid (HNO_3) vapour, giving rise to the remarkable reduction of sheet resistance.[42] The downshift of Fermi level of graphene also increases the junction height and accelerates the collection of photo-induced carriers.

The assembled photovoltaic devices were evaluated under the illumination of simulated AM 1.5G solar spectrum at 100 mW/cm^2. Considering the balance between conductivity and transparency, 3-layer graphene films were used as front electrodes. Ultrathin c-Si substrates of 40 μm were adopted due to the compromise of flexibility and light absorption. Figure 2c depicts current density *versus* voltage (*J-V*) curves of a typical device with and without HNO_3 doping in the dark, indicating the superior diode rectification behavior of the device by the good formation of heterojunction. Furthermore, the diode ideality factor (*n*) can be deduced to be 2.79 before doping and 2.31 after doping from the inset in Figure 2c, from

which it is inferred that the charge recombination is suppressed due to the decease of series resistance (R_s) of the device *via* HNO_3 doping. Figure 2d shows the photovoltaic characteristics of a typical graphene (3-layer)/P3HT (10 nm)/c-Si (40 μm) heterojunction solar cell in the flat configuration. The pristine device displays a short circuit current density (J_{sc}) of 20.50 mA/cm^2, an open circuit voltage (V_{oc}) of 0.55 V, and a fill factor (FF) of 0.52, yielding a PCE of 5.93%. After HNO_3 doping, the V_{oc} remains unchanged, while J_{sc} and FF are dramatically improved to 24.28 mA/cm^2 and 0.63, respectively, giving rise to an enhanced PCE of 8.42%. We ascribe the enhancement to the improved conductivity of graphene and consequently higher junction quality after doping. From EQE spectra in Figure 2e, it is observed that the EQE value is enhanced over wide wavelength region after HNO_3 doping, which is consistent with the photovoltaic measurements in Figure 2d. The EQE spectrum of the doped device shows a valley structure around 600 nm. This can be attributed to the light absorption of P3HT at this wavelength range; the inferior conductivity of P3HT will prevent the efficient hole transport from n-type c-Si to graphene, resulting in a performance degradation. Therefore, an optimum P3HT layer thickness of about 10 nm was selected in this study. In control experiment, device without P3HT layer was also measured (Figure S2, Supporting Information), showing an inferior device performance. This result coincides with above mentioned energy band analysis and expectations.

To elucidate the effect of ultrathin c-Si thickness on the device performance of the graphene/c-Si heterojunction solar cells, we fabricated the devices with varied thicknesses of 10, 20, and 40 μm, respectively. For better comparison, 3-layer graphene films were used for all devices. Figure 3a depicts the photovoltaic performance of the heterojunction solar cells with varied c-Si thickness under AM 1.5G illumination. Both J_{sc} and V_{oc} decrease as the thickness of ultrathin c-Si is decreased from 40 μm to 10 μm. For the 40 μm-thick ultrathin c-Si based device, the J_{sc} and V_{oc} are 22.86 mA/cm^2 and 0.55, leading to a PCE of 5.06% before HNO_3 doping, while the J_{sc}, V_{oc}, PCE decrease to18.86 mA/cm^2, 0.50 V, 3.45% and 12.06 mA/cm^2, 0.45 V, 1.96% for 20 μm- and 10 μm-thick ultrathin c-Si based devices, respectively. The drop of device performance is mainly attributed to the inadequate light absorption when the thickness of ultrathin c-Si substrate reduces down, which is observed from the absorption spectra of ultrathin c-Si in Fig. 1e. Once HNO_3 treatment was applied, the performances of all tested solar cells were

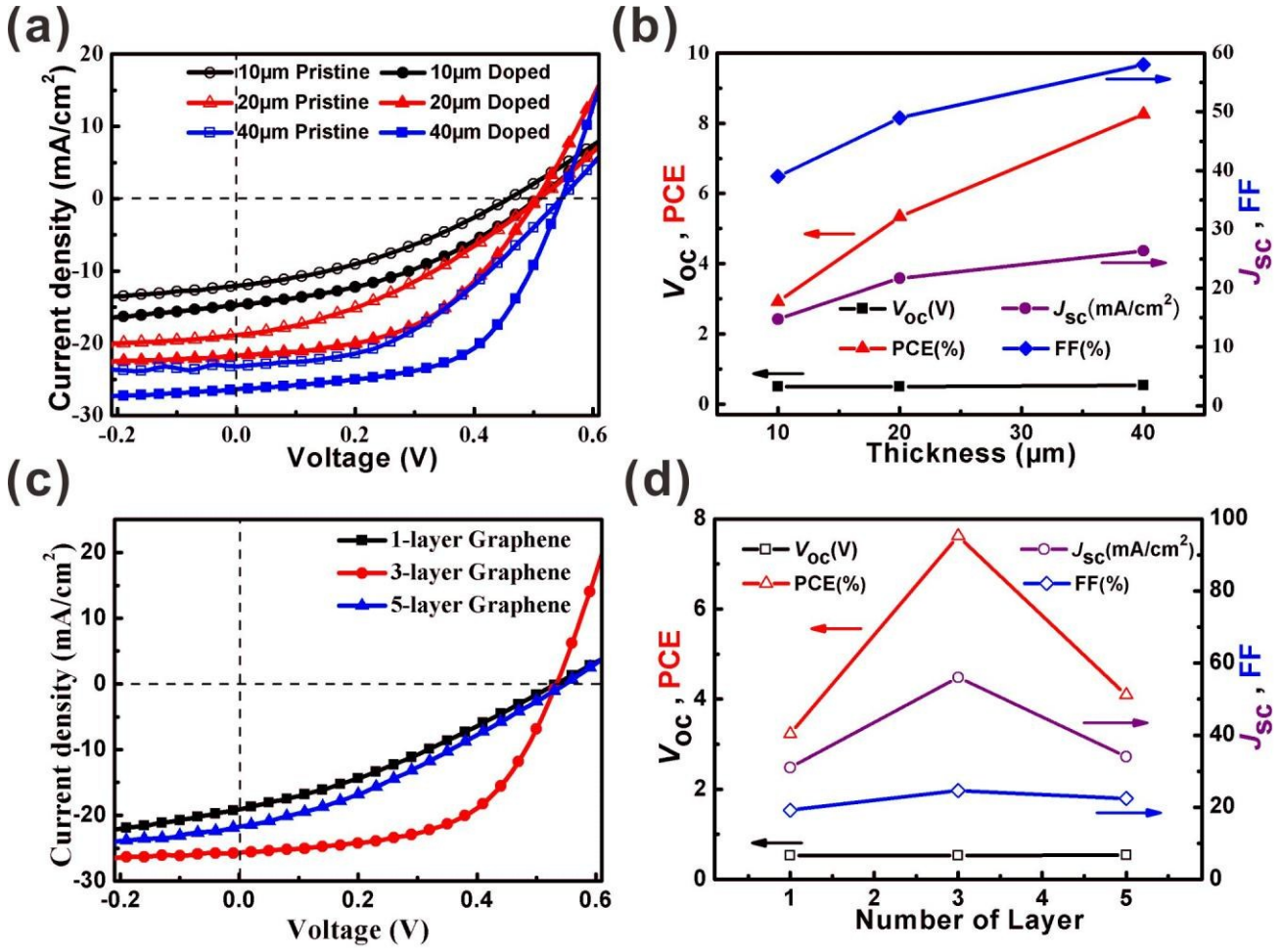

Figure 3. Electric output characteristics of the flexible graphene/ultrathin c-Si heterojunction solar cells. (a) *J-V* curves with c-Si substrate thickness of 10, 20, and 40 μm, respectively. (b) Plots of main device parameters as a function of c-Si thickness. (c) *J-V* curves of the devices with various graphene layer number. The thickness of c-Si was 40 μm. (d) Plots of main device parameters as a function of graphene layer number.

Journal Name

ARTICLE

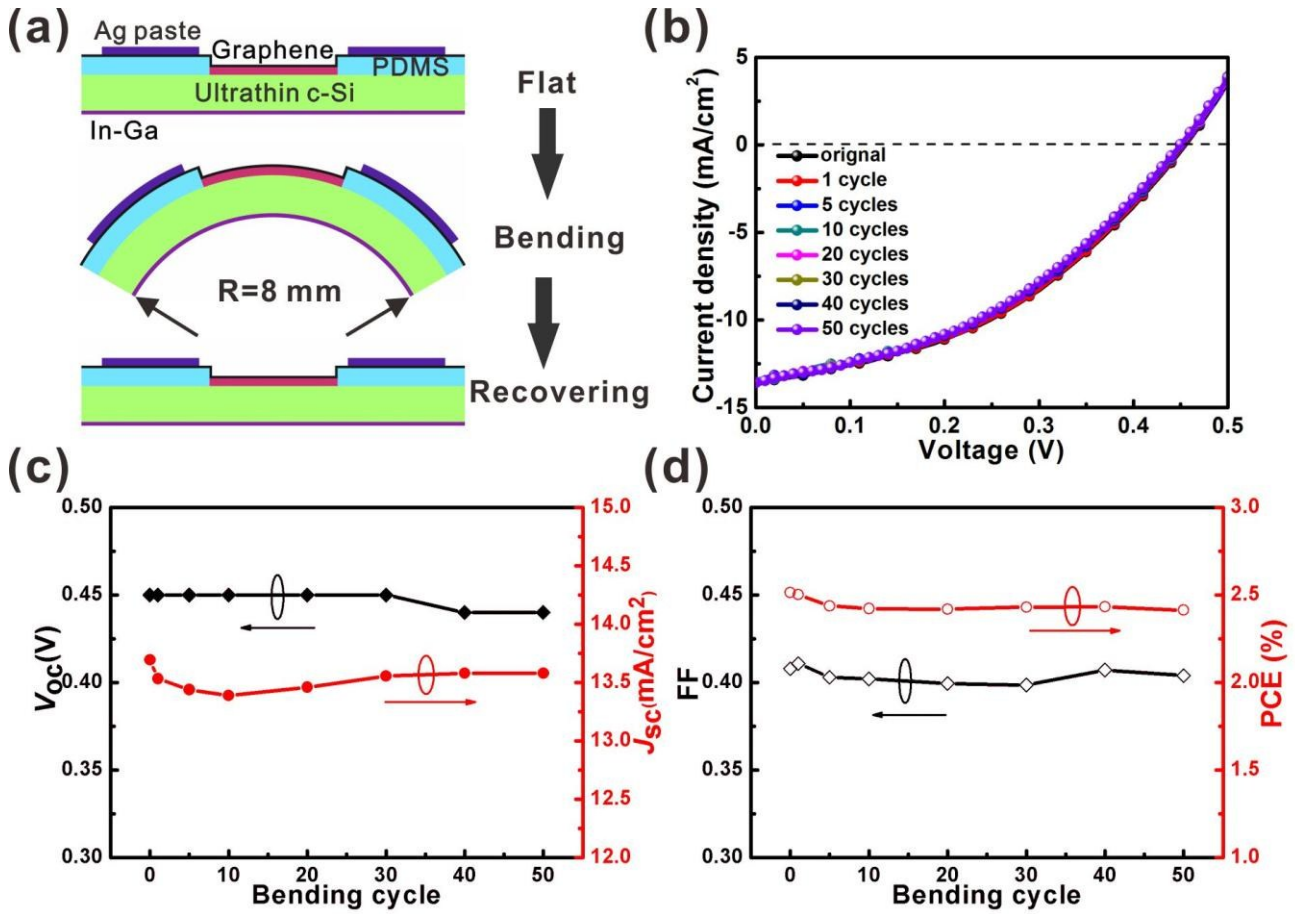

Figure 4. (a) Schematic illustration of the measurement configuration for bending test. (b) *J-V* curves of the graphene/ultrathin c-Si solar cell measured under various bending cycles. Dependence of (c) V_{oc}, J_{sc} and (d) FF, PCE on the bending cycle.

enhanced effectively, as presented in Fig. 3a. However, the trend of device performance after doping is similar with that before doping. On the other hand, to reveal how the layer number of graphene affects the photovoltaic characteristics, we investigated the device performance at various graphene layer numbers, while the thickness of ultrathin c-Si substrates was fixed at 40 μm. Figure 3c shows the typical *J-V* curves of the solar cells after HNO_3 doping, and the relation of main device parameters with the graphene layer number is plotted in Figure 3d. It is found that the device performance strongly depends on the graphene layer number; V_{oc} slightly increases from 0.50 V for 1-layer graphene to 0.53 V for 3-layer graphene, while J_{sc} and FF are significantly enhanced from 21.76 mA/cm^2 and 0.31 for 1-layer graphene to 24.66 mA/cm^2 and 0.56 for 3-layer graphene. As a result, the PCE of the 3-layer graphene based device reaches 7.61%, which is more than twice of that for the 1-layer graphene based device (3.27%). The enhancement in sheet conductivity as well as the work function of multi-layer graphene films could be responsible for this result. However, we note that the device consisting of 5-layer graphene exhibits an obvious degradation of performance, because of the reduced optical transmittance of the thick graphene film, as shown in Figure 1i.

Owing to the large flexibility of ultrathin c-Si as well as graphene film, the graphene/ultrathin c-Si heterojunctions possess great potential for flexible solar cell applications. A new batch of graphene (3-layer)/c-Si (15 μm) devices were measured under bending condition at a fixed bending radius of 8 mm without HNO_3 doping (Figure 4a). As presented in Figure 4b, the photovoltaic characteristics of the device shows negligible change after one bending cycle, revealing the excellent flexibility of the device. To better understand the mechanical flexibility, we also increased the bending cycles to 50 times by repeating the bending-recovering process. It is encouraging that our graphene/ultrathin c-Si solar cells show a good durability; the *J-V* curves of the device under different

Table1. Electric output characteristics of the graphene/ultrathin c-Si heterojunction solar cells with varied c-Si thickness and graphene layer number.

Device Types	V_{OC} (V)		J_{SC} (mA/cm^2)		FF		PCE (%)	
	pristine	doped	pristine	doped	pristine	doped	pristine	doped
10 μm	0.45	0.50	12.06	14.73	0.36	0.39	1.96	2.92
20 μm	0.50	0.50	18.86	21.70	0.36	0.49	3.45	5.34
40 μm	0.54	0.54	22.86	26.37	0.41	0.58	5.06	8.26
1L-Gr	0.51	0.53	10.30	19.19	0.22	0.31	1.23	3.23
3L-Gr	0.50	0.53	17.61	24.66	0.23	0.56	2.11	7.61
5L-Gr	0.54	0.54	13.80	22.24	0.23	0.34	1.42	4.09

bending cycles almost overlap with each other. Figure 4c and d plot the relation of the photovoltaic parameters with bending cycles. The J_{sc} and V_{oc} of the graphene/c-Si heterojunction solar cell decreases gently from 13.69 mA/cm^2 and 0.45 V to 13.58 mA/cm^2 and 0.44 V after 50 bending cycles, while the change in FF almost is nearly invisible. As a result, the PCE decreases slightly from 2.51% to 2.41%. The results unambiguously demonstrate the excellent flexibility as well as high durability of the graphene/ultrathin c-Si heterojunction solar cells.

Conclusions

In summary, we developed flexible graphene/silicon heterojunction solar cells by using ultrathin c-Si as substrates. By performing surface passivation on Si, inserting a layer of P3HT as an electron blocking layer, and controlling the layer number and doping of graphene, we demonstrated a PCE of 8.42% for 40 μm-thick c-Si based solar cell. The devices exhibited excellent flexibility and durability; the performance remained unchanged at a bending radius of 8 mm and the device could sustain the bending cycles up to 50. Enormous improvements on the device performance can be envisioned by further enhancing the light-harvest of ultrathin c-Si substrates using silicon nanostructures, anti-reflection coatings, or metallic nanoparticles.[43-46] In addition, the effective device area of the graphene/ultrathin c-Si heterojunction solar cell is about 0.13 cm^2, which is still smaller than the conventional Si p-n junction solar cells (>1 cm^2). The relatively small area of the devices is mainly attributed to the limit of graphene conductivity. Increasing the device area, but without improving the conductivity of graphene film, will lead to the degradation of device performance. In principle, the device area could be further increased by adding a mesh electrode on graphene or using metallic nanowires to enhance the conductivity of graphene. Given the high flexibility and solution process capability, it is expected that the graphene/ultrathin c-Si heterojunction solar cells will have important applications for future low-cost, mechanically flexible, high performance solar cells.

Acknowledgements

This work was supported by the National Basic Research Program of China (No. 2012CB932400), the Major Research Plan of the National Natural Science Foundation of China (Nos. 91233110, 91333208), the National Natural Science Foundation of China (Nos. 51172151, 51173124, 51401138), the Natural Science Foundation of Jiangsu Province (No. BK20131162), Project Funded by China Postdoctoral Science Foundation (No. 2014M551653), and a Project Funded by the Priority Academic Program Development of Jiangsu Higher Education Institutions. This work is sponsored by Qing Lan Project.

Notes and references

1 Q. F. Lin, H. T. Huang, Y. Jing, H. Y. Fu, P. C. Chang, D. D.Li, Y. Yao and Z. Y. Fan, *J. Mater. Chem. C* . 2014, **2**,1233-1247.

2 S. Jeong, M. D. McGehee and Y. Cui, *Nat. Commun.*, 2013, **4**, 2950.

3 D. H. Lee, J. Y. Kwon, S. Maldonado, A. Tuteja and A. Boukai, *Nano Lett.*, 2014, **14**, 1961-1967.

4 J. L. Cruz-Campa, M. Okandan, P. J. Resnick, P. Clews, T. Pluym, R. K. Grubbs, V. P. Gupta, D. Zubia and G. N. Nielson, *Sol. Energy Mater. Sol. Cells*, 2011, **95**, 551-558.

5 J. Zhang, T. Song, X. L. Shen, X. G. Yu, S. T. Lee and B. Q. Sun, *ACS Nano*, 2014, **8**, 11369-11376.

6 C. Berge, M. Zhu, W. Brendle, M. B. Schubert and J. H. Werner, *Sol. Energy Mater. Sol. Cells*, 2006, **90**, 3102-3107.

7 C. S. Solanki, R. R. Bilyalov, J. Poortmans, J. Nijs and R. Mertens, *Sol. Energy Mater. Sol. Cells*, 2004, **83**, 101-113.

8 J. S. Yoon, A. J. Baca, S.I. Park, P. Elvikis, J. B. Geddes, L.Li, R. H. Kim, J. L. Xiao, S. D. Wang, T. H. Kim, M. J. Motala, B. Y. Ahn, E. B. Duoss, J. A. Lewis, R. G. Nuzzo, P. M. Ferreira, Y. Huang, A. Rockett and J. A. Rogers, *Nat. Mater.*, 2008, 7, 907-915.

9 K. J. Yu, L. Gao, J. S. Park, Y. R. Lee, C. J. Corcoran, R. G. Nuzzo, D. Chanda and J. A. Rogers, *Adv. Energy Mater.*, 2013, **3**, 1401-1406.
10 S. W. Bedell, D. Shahrjerdi, B. Hekmatshoar, K. Fogel, P. A. Lauro, J. A. Ott, N. Sosa and D. Sadana, *IEEE J. Photovoltaics*, 2012, **2**, 141-147.
11 S. Saha, M. M. Hilali, E. U. Onyegam, D. Sarkar, D. Jawarani, R. A. Rao, L. Mathew, R. S. Smith, D. Xu, U. K. Das, B. Sopori and S. K. Banerjee, *Appl. Phys. Lett.*, 2013, **102**, 163904.
12 S. Wang, B. D. Weil, Y. Li, K. X. Wang, E. Garnett, S. Fan and Y. Cui, *Nano Lett.*, 2013, **13**, 4393-4398.
13 S. Thiyagu, C. C. Hsueh, C. T. Liu, H. J. Syu, T. C. Lin and C. F. Lin, *Nanoscale*, 2014, **6**, 3361-3366.
14 H. H. Sun, J. Q. Wei, Y. Jia, X. Cui, K. L. Wang and D. h. Wu, *Nanoscale Res. Lett.*, 2014, **9**, 514-514.
15 M. Sharma, P. R. Pudasaini, F. Ruiz-Zepeda, D. Elam and A. A. Ayon, *ACS Appl. Mater. Interfaces*, 2014, **6**, 4356-4363.
16 X. Wang, L. J. Zhi and K. Müllen, *Nano Lett.*, 2008, **8**, 323-327.
17 K. S. Kim, Y. Zhao, H. Jang, S. Y. Lee, J. M. Kim, K. S. Kim, J. H. Ahn, P. Kim, J. Y. Choi and B. H. Hong, *Nature*, 2009, **457**, 706-710.
18 M. He, J. H. Jung, F. Qiu and Z. Q. Lin, *J. Mater. Chem.*, 2012, **22**, 24254-24264.
19 X. Huang, Z. Y. Zeng, Z. X. Fan, J. Q. Liu and H. Zhang, *Adv. Mater.*, 2012, **24**, 5979-6004.
20 D. D. Nguyen, N. H. Tai, Y. L. Chueh, S. Y. Chen, Y. J. Chen, W. S. Kuo, T. W. Chou, C. S. Hsu and L. J. Chen, *Nanotechnology*, 2011, **22**, 295606.
21 L. H. Zeng, M. Z. Wang, H. Hu, B. Nie, Y. Q. Yu, C. Y. Wu, L. Wang, J. G. Hu, C. Xie, F. X. Liang and L. B. Luo, *ACS Appl.Mater.Interfaces*, 2013, **5**, 9362-9366.
22 X. S. Li, W. W. Cai, J. H. An, S. Y. Kim, J. H. Nah, D. X. Yang, R. Piner, A. Velamakanni, I. Jung, E. Tutuc, S. K. Banerjee, L. Colombo and R. S. Ruoff, *Science*, 2009, **324**, 1312-1314.
23 S. K. Bae, H. K. Kim, Y. B. Lee, X. F. Xu, J. S. Park, Y. Zheng, J. Balakrishnan, T. Lei, H. Ri Kim, Y. I. Song, Y. J. Kim, K. S. Kim, B. Ozyilmaz, J. H. Ahn, B. H. Hong and S. Iijima, *Nat. Nanotech.*, 2010, **5**, 574-578.
24 A. Badmaev, Y. Che, Z. Li, C. Wang and C. W. Zhou, *ACS Nano*, 2012, **6**, 3371-3376.
25 C. L. Hsu, C. T. Lin, J. H. Huang, C. W. Chu, K. H. Wei and L. J. Li, *ACS Nano*, 2012, **6**, 5031-5039.
26 A. Kuruvila, P. R. Kidambi, J. Kling, J. B. Wagner, J. Robertson, S. Hofmann and J. Meyer, *J. Mater.Chem. C*, 2014, **2**, 6940-6945.
27 L. B. Luo, J. J. Chen, M. Z. Wang, H. Hu, C. Y. Wu, Q. Li, L. Wang, J. A. Huang and F. X. Liang, *Adv. Funct. Mater.*, 2014, **24**, 2794-2800.
28 Y. Z. Chen, H. Medina, H. C. Lin, H. W. Tsai, T. Y. Su and Y. L. Chueh, *Nanoscale*, 2015, **7**, 1678-1687.
29 Y. Ye and L. Dai, *J. Mater. Chem.*, 2012, **22**, 24224-24229.
30 X. M. Li, H. W. Zhu, K. L. Wang, A. Y. Cao, J. Q. Wei, C. Y. Li, Y. Jia, Z. Li, X. Li and D. H. Wu, *Adv. Mater.*, 2010, **22**, 2743-2748.
31 T. T. Feng, D. Xie, Y. X. Lin, H. M. Zhao, Y. Chen, H. Tian, T. L. Ren, X. H. Li, Z. Li, K. L. Wang, D. H. Wu and H. W. Zhu, *Nanoscale*, 2012, **4**, 2130-2133.
32 X. C. Miao, S. Tongay, M. K. Petterson, K. Berke, A. G. Rinzler, B. R. Appleton and A. F. Hebard, *Nano Lett.*, 2012, **12**, 2745-2750.
33 X. Z. Zhang, C. Xie, J. S. Jie, X. W. Zhang, Y. M. Wu and W. J. Zhang, *J. Mater. Chem. A.*, 2013, **1**, 6593-6601.
34 C. Xie, X. Z. Zhang, Y. M. Wu, X. J. Zhang, X. W. Zhang, Y. Wang, W. J. Zhang, P. Gao, Y. Y. Han and J. S. Jie, *J. Mater. Chem. A.*, 2013, **1**, 8567-8574.
35 Y. M. Wu, X. Z. Zhang, J. S. Jie, C. Xie, X. W. Zhang, B. Q. Sun, Y. Wang and P. Gao, *J. Phys. Chem. C*, 2013, **117**, 11968-11976.
36 E. Z. Shi, H. B. Li, L. Yang, L. H. Zhang, Z. Li, P. X. Li, Y. Y. Shang, S. T. Wu, X. M. Li, J. Q. Wei, K. L. Wang, H. W. Zhu, D. H. Wu, Y. Fang and A. Y. Cao, *Nano Lett.*, 2013, **13**, 1776-1781.
37 Y. Song, X. M. Li, C. Mackin, X. Zhang, W. J. Fang, T. Palacios, H. W. Zhu and J. Kong, *Nano Lett.*, 2015, **15**, 2104-2110.
38 Y. Wang, S. W. Tong, X. F. Xu, B. Özyilmaz and K. P. Loh, *Adv. Mater.*, 2011, **23**, 1514-1518.
39 N. Alderman, L. Danos, M. C. Grossel and T. Markvart, *RSC Adv.*, 2012, **2**, 7669-7672.
40 F. T. Zhang, D. Liu, Y. F. Zhang, H. X. Wei, T. Song and B. Q. Sun, *ACS Appl. Mater. Interfaces*, 2013, **5**, 4678-4684.
41 S. Maldonado, D. Knapp and N. S. Lewis, *J. Am. Chem. Soc.*, 2008, **130**, 3300-3301.
42 H. T. Liu, Y. Q. Liu and D. B. Zhu, *J. Mater. Chem.*, 2011, **21**, 3335-3345.
43 Y. F. Li, M. C. Li, R. K. Li, P. F. Fu, L. H. Chu and D. D. Song, *Appl. Phys. Lett.*, 2015, **106**, 091908.
44 K. H. Tsui, Q. F. Lin, H. T. Chou, Q. P. Zhang, H. Y. Fu, P. F. Qi and Z. Y. Fan, *Adv. Mater.*, 2014, **26**, 2805-2811.
45 Z. Y. Feng, C. Jiang, Y. He, S. Chu, G. Chu, R. F. Peng and D. D. Li, *Adv. Opt. Mater*, 2014, **2**, 1174-1180.
46 S. -F. Leung, Q. P. Zhang, F. Xu, D. L. Yu, J. Ho, D. D. Li, Z. Y. Fan, *J. Phy. Chem. L.* 2014, **5**, 1479-1495.

We demonstrate the construction of flexible graphene/ultrathin c-Si heterojucntion solar cells with excellent flexibility and durability.

Kaiqun Ruan, Ke Ding, Yuming Wang, Senlin Diao, Zhibin Shao, Xiujuan Zhang and Jiansheng Jie**

Title: **Flexible Graphene/Silicon Heterojunction Solar Cells**

ToC figure: